Geophysical Research Letters

RESEARCH LETTER
10.1029/2019GL082929

Improved Earth Oblateness Rate Reveals Increased Ice Sheet Losses and Mass-Driven Sea Level Rise

B. D. Loomis[1], K. E. Rachlin[2], and S. B. Luthcke[1]

[1]NASA Goddard Space Flight Center, Greenbelt, MD, USA, [2]KBRwyle, Greenbelt, MD, USA

Key Points:
- New satellite laser ranging C_{20} solution reveals larger Antarctic and Greenland ice mass losses and mass-driven sea level rise
- The new C_{20} result improves closure of the global mean sea level budget and agreement with an independent Antarctic ice mass assessment
- We recommend this new product for replacing the GRACE C_{20} values for science applications

Correspondence to:
B. D. Loomis,
bryant.d.loomis@nasa.gov

Citation:
Loomis, B. D., Rachlin, K. E., & Luthcke, S. B. (2019). Improved Earth oblateness rate reveals increased ice sheet losses and mass-driven sea level rise. *Geophysical Research Letters*, *46*. https://doi.org/10.1029/2019GL082929

Received 21 MAR 2019
Accepted 29 MAY 2019
Accepted article online 4 JUN 2019

Abstract Satellite laser ranging (SLR) observations are routinely applied toward the estimation of dynamic oblateness, C_{20}, which is the largest globally integrated component of Earth's time-variable gravity field. Since 2002, GRACE and GRACE Follow-On have revolutionized the recovery of higher spatial resolution features of global time-variable gravity, with SLR continuing to provide the most reliable estimates of C_{20}. We quantify the effect of various SLR processing strategies on estimating C_{20} and demonstrate better signal recovery with the inclusion of GRACE-derived low-degree gravity information in the forward model. This improved SLR product modifies the Antarctic and Greenland Ice Sheet mass trends by −15.4 and −3.5 Gt/year, respectively, as compared to CSR TN11, and improves global mean sea level budget closure by modifying sea level rise by +0.08 mm/year. We recommend that this new C_{20} product be applied to RL06 GRACE data products for enhanced accuracy and scientific interpretation.

1. Introduction

For more than four decades, satellite laser ranging (SLR) has been utilized to monitor changes in the Earth's dynamic oblateness, C_{20} (this term is often described instead by J_2, which differs from C_{20} by a constant factor: $J_2 = -C_{20}\sqrt{5}$). As C_{20} is the largest component of Earth's time-variable gravity (TVG) field, its accurate recovery is of great importance for recovering regional mass variability and understanding changes in the Earth climate system. Centuries-long linear trends in C_{20} are caused by glacial isostatic adjustment (GIA), which is the ongoing solid Earth response to significant land ice losses since the last glacial maximum. Other temporal variability in C_{20} is primarily the result of water mass exchanges between the high latitude and midlatitude regions, dominated in recent years by the melting of the Greenland Ice Sheet (GIS) and Antarctic Ice Sheet (AIS; Nerem & Wahr, 2011) and the associated heterogeneous changes in sea level (Hsu & Velicogna, 2017).

With its launch in March 2002, GRACE initiated a new era for monitoring global water mass fluxes, providing monthly measurements of TVG to a spatial resolution of 300–500 km (Luthcke et al., 2013; Wahr et al., 2006). After a relatively short gap between missions, the successful launch of GRACE Follow-On (GRACE-FO) in May 2018 is currently extending the time series of this unique data set. The standard Level-2 GRACE and GRACE-FO data product is a series of spherical harmonic coefficients estimated monthly to at least degree and order 60. It became apparent early in the mission that the GRACE-derived C_{20} estimates were unreliable, as they contained an unexpected ~161-day periodic signal, and the trends differed from SLR-derived values. Various explanations have been proposed for the erroneous 161-day signal, including aliasing of the S2 ocean tide (Chen et al., 2009; Ray & Luthcke, 2006; Seo et al., 2008), and cross-track accelerometer errors from thermal effects driven by β', the angle between the Sun and the orbital plane (Cheng & Ries, 2017; Klinger & Mayer-Gürr, 2016). Regardless of the error source, it has become standard practice to replace the GRACE C_{20} estimates with values obtained by SLR in order to ensure the proper scientific application of GRACE data products (Cheng et al., 2013). The level 3 global mascon products provided by the NASA Goddard Space Flight Center (GSFC), the Jet Propulsion Laboratory (JPL), and the Center for Space Research at the University of Texas (CSR) also utilize this C_{20} replacement approach (Loomis et al., 2019; Save et al., 2016; Watkins et al., 2015).

In addition to the accurate recovery of C_{20}, SLR-derived low-degree gravity solutions have a much longer and continuous data record, providing valuable TVG information prior to GRACE and during the gap between GRACE and GRACE-FO. The utility of these observations continues to drive advancements in SLR data processing for improving the accuracy of the recovered low-degree gravity coefficients (Bloßfeld et al., 2015;

Table 1
Summary of Various SLR and Combined SLR/GRACE Gravity Solutions

Solution	Satellites	Weights	SLR arc	TVG	Gravity coef.
GSFC recommended	5-SLR	CSR	[a]28/7 days	Yes	$5 \times 5; C_{61}/S_{61}$
GSFC TN11-like	5-SLR	CSR	3.5 days	No	$5 \times 5; C_{61}/S_{61}$
CSR TN11	5-SLR	CSR	3 days	No	$5 \times 5; C_{61}/S_{61}$
AIUB	[b]9-SLR	AIUB	[a]10/1 days	Yes	6×6
DGFI	[b]10-SLR	DGFI	7 days	Yes	6×6
GRGS	4-SLR	[c]n/a	5 days	Yes	2×2
CSR combined	5-SLR+GRACE	CSR	3 days	No	60×60
GRGS combined	4-SLR+GRACE	[c]n/a	[a]10/5 days	Yes	90×90

Note. SLR = satellite laser ranging; TVG = time-variable gravity; GSFC = Goddard Space Flight Center; CSR = Center for Space Research at the University of Texas; AIUB = Astronomisches Institut, Universität Bern; DGFI = Deutsches Geodätisches Forschungsinstitut, Technische Universitlät München; GRGS = Groupe de Recherche de Géodésie Spatiale.
[a]The first number is the LAGEOS-1/2 arc length; the second is for all others. [b]LARES contributions begin in February 2012. [c]Not provided.

Cheng & Ries, 2017; Sośnica et al., 2015). Several studies have sought to infer changes in the GIS and AIS prior to the GRACE mission, by processing or analyzing SLR gravity solutions in conjunction with GRACE-derived TVG information (Bonin et al., 2018; Nerem & Wahr, 2011; Talpe et al., 2017). Other studies have combined GRACE and SLR observations at the normal equation level in an effort to produce a more optimum solution, with Lemoine et al. (2007) and Sośnica et al. (2015) claiming improved C_{20} estimates with the combined approach, while Cheng and Ries (2017) recommend their SLR-only solution.

In this study we present a systematic approach toward the development of a new C_{20} solution. The comparative analyses focus on the C_{20} trend, as significant discrepancies exist between previously published results, and the trend alone has an important impact on GRACE-derived changes of global mean sea level (GMSL) and ice mass in the AIS, and GIS. In addition to our own C_{20} solution (GSFC), we analyze and discuss the recent results from CSR (Cheng & Ries, 2017); the Astronomisches Institut, Universität Bern (AIUB; Sośnica et al., 2015); the Centre National d'Etudes Spatiales/Groupe de Recherche de Géodésie Spatiale (GRGS; Lemoine et al., 2018), and the Deutsches Geodätisches Forschungsinstitut, Technische Universität München (DGFI; Bloßfeld et al., 2015). We process the SLR observations with a variety of strategies in order to understand the differences in the various C_{20} solutions, with the goal of converging on a recommended methodology. This systematic approach quantifies the effects of the data reduction arc length, SLR tracking data weights, GRACE-derived forward models, and expansion of the estimated gravity field. We demonstrate that the inclusion of GRACE-derived TVG in the SLR data reduction forward modeling is the most important design choice, owing to the high correlation between coefficients C_{20} and C_{40} in SLR-only estimates. The CSR C_{20} product commonly used for replacing GRACE C_{20} does not currently utilize this forward modeling strategy, and we recommend that GRACE users apply the new GSFC C_{20} solution for improved application and scientific interpretation of GRACE and GRACE-FO data products.

2. Data and Methods

2.1. Independent SLR C_{20} Solutions

The primary motivation for this work is to understand the disparate C_{20} trends of previously published results, in order to provide the science community with a new optimal C_{20} solution for replacing GRACE values and for extending TVG studies beyond the spans of the dedicated TVG missions. To that end, we begin by summarizing published SLR-derived C_{20} solutions, highlighting the key design choices for each. As shown in Table 1, these design parameters are the number of selected satellites (including if it is a combined solution with GRACE), the data weights assigned to each SLR satellite, the length of the SLR data reduction arcs, the inclusion or exclusion of TVG in the forward model, and the set of estimated gravity spherical harmonic coefficients.

Though different numbers of SLR satellites are applied in the various solutions, in practice they are quite similar in terms of information content. All GSFC solutions use the same five satellite set as CSR: LAGEOS

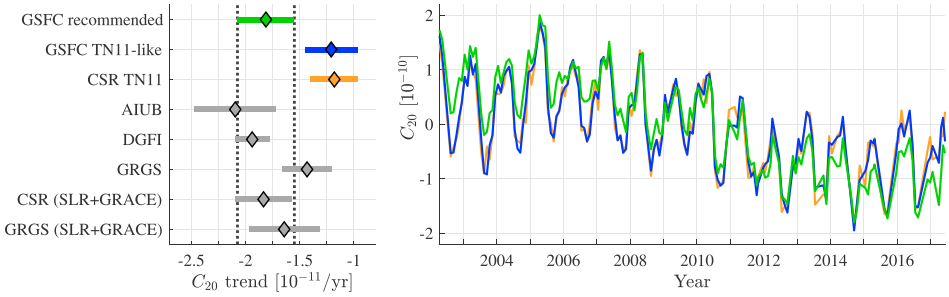

Figure 1. (Left) C_{20} trends for various solutions with 95% uncertainties are shown for September 2002 to June 2013. The vertical dashed lines denote the 95% uncertainties for the recommended solution. (Right) The C_{20} solution over the GRACE mission span is shown for the GSFC recommended solution (green), the GSFC solution with similar setup to TN11 (blue), and the CSR TN11 solution (orange). GSFC = Goddard Space Flight Center; CSR = Center for Space Research at the University of Texas; GMSL = global mean sea level; AIUB = Astronomisches Institut, Universität Bern; DGFI = Deutsches Geodätisches Forschungsinstitut, Technische Universität München; SLR = satellite laser ranging.

1 and 2, Starlette, Stella, and AJISAI (defined hereafter as CSR5). The 9-satellite AIUB solution includes CSR5, LARES, Larets, BLITS, and Beacon-C, while the 10-satellite DGFI uses CSR5, LARES, Larets, BLITS, and Etalon 1 and 2. LARES was launched in 2012, so only contributes to a small portion of the time span common to all data sets (September 2002 to June 2013). Sośnica et al. (2015) conclude that up until 2012, their solution is primarily driven by CSR5, as Larets and BLITS add little information beyond that provided by Stella, and Beacon-C is strongly down-weighted. Examination of the satellite weights applied by Bloßfeld et al. (2015) reveals a similar situation, in that the CSR5 satellites are up-weighted relative to the others with a similar altitude. We also note that Cheng and Ries (2017) observed negligible changes to the recovered C_{20} trend when using additional satellites to CSR5. The GRGS solution excludes AJISAI from CSR5, which is expected to have little effect on C_{20}, as LAGEOS-1/2 data are the primary driver of the recovered zonal coefficients (Sośnica et al., 2015). For the data weights, CSR applies an iterative procedure where the weights are estimated as a part of the solution until convergence occurs (Cheng & Ries, 2017), and DGFI uses the variance component estimation algorithm summarized in Böckmann et al. (2010). The process of AIUB data weight selection is not described by Sośnica et al. (2015) and the GRGS weights are not readily available. Another key design choice is the length of the data arcs in which we process the SLR measurements and estimate arc-specific parameters (e.g., satellite orbits and measurement biases). For all considered solutions, the normal equations for each arc are later combined to form monthly estimates of the gravity coefficients, but as noted by Cheng and Ries (2017), the selection of shorter arcs may inhibit the ability to fully recover C_{20}. For the previously published solutions, the arc length of the higher altitude satellites (LAGEOS-1/2) span from 3 to 7 days, while the lower-altitude SLR satellites have arcs from 1 to 7 days.

There are important differences between solutions regarding the a priori background gravity models applied in the SLR measurement processing. CSR is the only solution that does not apply any time dependence in the gravity model. AIUB and GRGS use different versions of the EIGEN mean gravity models (Förste et al., 2016), which are defined by a high-resolution bias (mean), plus a lower-resolution expansion of trend and periodic components of the TVG. AIUB also applies time dependence by defining the monthly TVG GRACE solution of (Meyer et al., 2012) as their background model. It is important to note that different versions of the atmospheric and ocean dealiasing (AOD) products (Flechtner, 2007) were used in the data processing for the different solutions, and this has been fully accounted for so that all results are consistent with the RL06 AOD product. Finally, the solutions also differ by the selected spherical harmonic coefficients that they estimate. CSR estimates a 5×5 plus C_{61}/S_{61}, where the additional 6,1 terms improve the agreement between the SLR and GRACE solutions for C_{21}. AIUB produced both 6×6 and 10×10 solutions, with Sośnica et al. (2015) noting that LARES data are needed to provide meaningful information above degree 6. The C_{20} solutions are similar for both products, and we have chosen to present results for the 6×6 product. The DGFI solution is 6×6, and the GRGS solution is 2×2. We also analyze CSR and GRGS solutions that combine SLR and GRACE data at the normal equation level, with expansions of 60×60 and 90×90, respectively. We also note that CSR, AIUB, and GRGS coestimate geocenter (degree 1) while DGFI does not. All GSFC solutions discussed below do not estimate geocenter, but the results in Figure 1 show that the CSR solution is well replicated without it.

Table 2
Summary of C_{20} Trends for 2005–2015 for Various GSFC Solution Scenarios and CSR TN11

Solution	C_{20} trend (10^{-11} year^{-1})	ΔC_{20} (10^{-11} year^{-1})	ΔGMSL (mm/year)	ΔAIS (Gt/year)	ΔGIS (Gt/year)
GSFC					
Recommended	−2.38	—	—	—	—
3.5-day arcs	−2.32	−0.06	0.01	−1.4	−0.3
7-day arcs[a]	−2.33	−0.05	0.01	−1.2	−0.3
7-day; AIUB weights	−2.33	−0.05	0.01	−1.1	−0.3
7-day; DGFI weights	−2.33	−0.05	0.01	−1.3	−0.3
6 × 6 estimated	−2.52	0.14	−0.02	3.2	0.7
2 × 2 estimated	−2.32	−0.07	0.01	−1.5	−0.4
No atmospheric loading	−2.38	0.00	0.00	0.0	0.0
No TVG	−1.97	−0.41	0.05	−9.7	−2.2
No TVG; 3.5-day[b]	−1.74	−0.64	0.08	−15.2	−3.5
CSR					
TN11	−1.73	−0.65	0.08	−15.4	−3.5

Note. GSFC = Goddard Space Flight Center; CSR = Center for Space Research at the University of Texas; GMSL = global mean sea level; AIS = Antarctic ice sheet; GIS = Greenland ice sheet; AIUB = Astronomisches Institut, Universität Bern; DGFI = Deutsches Geodätisches Forschungsinstitut, Technische Universität München; TVG = time-variable gravity. The C_{20} trend fit 1–σ uncertainties are $\pm 0.06 \times 10^{-11}$ year^{-1} for both GSFC and CSR.
[a]The 7-day arc scenarios only modifies the arc-length of LAGEOS-1/2. [b]This is the "TN11-like" solution in Table 1 and Figure 1.

In section 3 we compare new GSFC C_{20} results to independent solutions over the time span common to all SLR products: September 2002 to June 2013. We also compare CSR and a suite of GSFC solution trends over January 2005 to December 2015, matching the common span of GRACE, Argo, and sea surface altimetry data, which directly measure the mass, steric, and total GMSL, respectively. These concurrent data sets facilitate the comparison of the various C_{20} solutions in terms of their impacts on closing the GMSL budget.

2.2. GSFC SLR Processing Models and Standards

Our nominal SLR strategy is largely built on the previous work of Lemoine et al. (2006), Zelensky et al. (2014), and Cheng and Ries (2017) and includes improved models and standards adopted by our group for producing our global GRACE mascon solutions (Loomis et al., 2019). As described above, our solution includes data from the higher altitude satellites LAGEOS 1 and 2, and lower-altitude satellites Starlette, Stella, and AJISAI.

We process the SLR measurements with a background gravity field defined by the sum of the static GOCO-05s model (Pail et al., 2010) and our own 10 × 10 TVG model. All TVG coefficients are described by the trend and seasonal model that best fits the CSR RL05 GRACE product, except for C_{20}, which fits a trend and periodic signals of 1, 0.5, and 18.6 years to the SLR-derived CSR TN07 (the previous version of the TN11 product). We note that only statistically significant model fits to the gravity coefficients are included (i.e., terms lacking significance are set to zero). Additional background models include the RL06 AOD1B (Flechtner, 2007), solid Earth tides (Petit & Luzum, 2010), ocean tides (Ray, 1999), and pole tide (Ries & Desai, 2017). We use the ITRF2014 station positions, which include postseismic deformation corrections where necessary. Additional station position corrections account for the solid Earth tide and ocean tidal loading (Petit & Luzum, 2010), and atmospheric loading (Petrov & Boy, 2004). Satellite-specific center-of-mass offsets are modeled after (Otsubo & Appleby, 2003; Otsubo et al., 2015), and we estimate station biases and satellite-specific arc parameters as described in Zelensky et al. (2014). For our nominal solution, Starlette, Stella, and AJISAI are processed individually in 7-day arcs, while the LAGEOS satellites are processed together in 28-day arcs (relative LAGEOS-1/2 weighting is handled by the assigned measurement standard deviation). The combined long-arc approach for LAGEOS follows the pre-1992 procedures in Lemoine et al. (2006) and improves the robustness of station bias estimates. These long data reduction arcs are supported by the estimation of along-track empirical accelerations every 3.5 days. The normal equations for all arcs in a given 28-day span are then combined and inverted to obtain the low-degree gravity estimates.

Table 1 summarizes the key differences in SLR processing strategies between the previously published solutions, while Table 2 details our systematic approach to quantifying the effects of each design permutation. These include variations in the data arc length, the assigned satellite data weights, the inclusion of TVG, and the expansion of the estimated gravity coefficients.

3. Results and Discussion

Figure 1 presents the results of the C_{20} trend comparison for the various solutions summarized in Table 1 and also compares the full time series over the GRACE mission span for the CSR TN11, GSFC recommended, and GSFC "TN11-like" solutions. The excellent agreement between CSR TN11- and GSFC TN11-like validates our ability to reproduce the CSR TN11 solution and establishes that the differences between our recommended solution and CSR are largely due to the different arc lengths and the application of TVG in the forward model. The relative importance of each design choice is further explored below. Examining the Figure 1 trends of the various products reveals that all of the independent SLR-only and SLR/GRACE combined solutions agree with the recommended GSFC solution within 95% uncertainties, except for CSR TN11, highlighting the importance of understanding which solution should be used in the application of GRACE data products.

The results presented in Table 2 summarize our efforts to fully quantify the effects of the various design parameters applied by the different SLR processing centers. In addition to computing the effect on the C_{20} trend, we also include the associated changes in the mass component of GMSL and the ice mass losses in AIS and GIS. The Δ values describe the difference to the recommended GSFC solution; for example, a negative ΔAIS value means that the recommended solution is more negative than the alternative solution.

Examination of the values in Table 2 reveals that the selected arc length, gravity field expansion, and TVG all have some effect on the recovered C_{20} trend, while the selected data weights and atmospheric loading effects are negligible (weighting effects are quantified by the three 7-day arc solutions). Considering the change in arc length alone, we observe the largest effect when reducing the length of the LAGEOS-1/2 arc lengths from 28 days to weekly (-0.05×10^{-11} year^{-1}), with much smaller differences between weekly and 3.5 days (-0.01×10^{-11} year^{-1}). It is interesting to note that the effect of the 3.5-day arc length is more pronounced when TVG is excluded (-0.23×10^{-11} year^{-1}) than when it is included (-0.06×10^{-11} year^{-1}). When modifying the nominal set of estimated coefficients, we observe a more pronounced effect when increasing the expansion to 6×6 ($+0.14\times10^{-11}$ year^{-1}) than when reducing to 2×2 (-0.07×10^{-11} year^{-1}). The results in Table 2 clearly demonstrate that the choice to include or exclude TVG in the forward model is the single largest determinant of the recovered C_{20} trend, where the combined effect of increased arc length and inclusion of TVG modifies the GMSL, AIS, and GIS trends by +0.08 mm/year, −15.2 Gt/year, and −3.5 Gt/year, respectively, effectively matching the differences to CSR TN11 of +0.08 mm/year, −15.4 Gt/year, and −3.5 Gt/year. We note that the results are fairly insensitive to the a priori C_{20} model, as a model based on the GRACE CSR RL06 C_{20} instead of the SLR-based model modified the recovered trend by only 5.9×10^{-15} year^{-1}.

The effects of gravity expansion and TVG forward models on the C_{20} solution is well explained by the high correlations that exist between C_{20} and the other estimated gravity coefficients. For the GSFC and CSR adjusted parameter set ($5\times5+C_{61}/S_{61}$), the only term with a significant correlation to C_{20} is C_{40} (defined as $\rho_{C_{40}}^{C_{20}}$). Our recommended solution has a $\rho_{C_{40}}^{C_{20}}$ of −0.46, with CSR reporting a similar correlation of −0.41. When estimating a full 6 × 6 gravity field, $\rho_{C_{40}}^{C_{20}}$ increases dramatically to −0.87. Our 7-day arc 6 × 6 solution has a $\rho_{C_{40}}^{C_{20}}$ of −0.97, which agrees well with the reported CSR value of −0.95 when C_{60} is adjusted. These significant increases in $\rho_{C_{40}}^{C_{20}}$, and the effect on the C_{20} trend (also observed by Cheng & Ries, 2017), provide strong support for excluding C_{60} from the parameter set. The results in Table 2 show that a full 6 × 6 expansion modifies the GSFC C_{20} trend by $+0.14\times10^{-11}$ year^{-1}, fully explaining the difference with DGFI ($+0.13\times10^{-11}$ year^{-1}) and half of the difference with AIUB ($+0.28\times10^{-11}$ year^{-1}) shown in Figure 1. While applying GRACE-derived TVG in the forward model has no effect on the actual correlation values, the effect of these high correlations on the C_{20} solution is significantly mitigated by processing the SLR data with the TVG. The significantly lower $\rho_{C_{40}}^{C_{20}}$ for GRACE-only solutions and the excellent agreement between independent GRACE C_{40} estimates both provide strong justification for including GRACE-derived TVG in the SLR data reduction modeling.

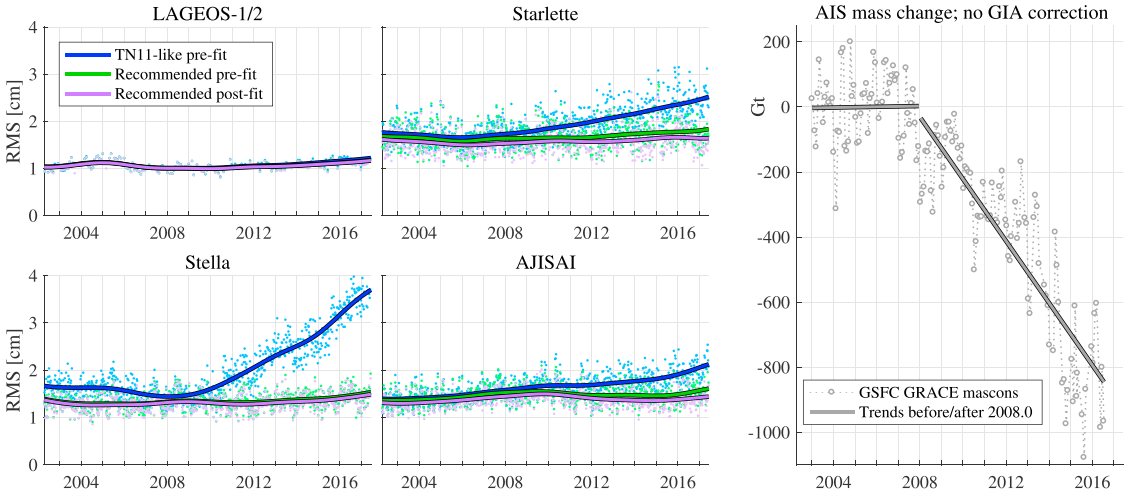

Figure 2. (Left) Prefit satellite laser ranging measurement residuals for the recommended setup that includes time-variable gravity in the forward model (green) and the "TN11-like" setup that does not (blue), along with the postfit residuals to the recommended low-degree solution (purple). (Right) Mass change in the Antarctic Ice Sheet (AIS) from GRACE Goddard Space Flight Center (GSFC) mascons v2.4 (Loomis et al., 2019) with no glacial isostatic adjustment (GIA) correction applied.

The benefit of modeling TVG is also demonstrated in Figure 2, which shows the large reduction in the long-term SLR measurement prefit (i.e., prior to adjusting gravity parameters) residuals when TVG is included in the forward model, and even further reductions for the postfit residuals. As expected, the magnitude of improvement is greatest for the lower-altitude satellites Starlette, Stella, and AJISAI. We note in Figure 2 that the large trend in the TN11-like prefit residuals for these satellites that begins in 2008–2009 corresponds to the timing of dramatic changes in GRACE-derived AIS mass. Due to its near-polar orbit (inclination = 98.6°), Stella exhibits the highest sensitivity to AIS variability. We also tested solution iteration in an effort to converge on the GSFC recommended solution without the use of GRACE TVG information. In that case, we defined the TVG model by the trend and periodic fits to the $5 \times 5 + C_{61}/S_{61}$ parameters estimated from the TN11-like setup. Solution iteration did not modify the result, confirming that the primary issue resolved with GRACE TVG is the correlation of parameters and not system nonlinearity.

Validating the C_{20} trend is challenging. While various studies have compared the annual components of length-of-day (LOD) observations to those derived by SLR/GRACE C_{20} solutions (Bourda, 2008; Jin et al., 2011; Yu et al., 2018), the geophysical impact of the C_{20} trend has not been as widely discussed. Perhaps the best independent validation of C_{20} trend estimates is to consider their effect on GMSL budget closure. Total GMSL variability has been continuously measured since 1992 with a series of sea surface altimetry satellites, and should equal the sum of the mass component measured by GRACE, and the steric component observed by a global network of profiling floats. Sufficient spatial coverage of the Argo float network for reliably measuring steric GMSL was achieved around 2005 (Leuliette & Willis, 2011), explaining 2005–2015 as our analysis period. For assessing the GMSL budget closure, we consider the recent international collaborative effort of the World Climate Research Programme (Group, WCRP Global Sea Level Budget, 2018), which presents a total GMSL trend of 3.70 ± 0.35 mm/year and full-depth steric trend of 1.31 ± 0.20 mm/year for their ensemble solutions from 2005–2015 (all uncertainties are 1–σ). To compute the mass component of GMSL, we use the CSR RL06 GRACE monthly gravity field product, apply a 300-km coastal buffer (Johnson & Chambers, 2013), and correct for the GIA model of Geruo et al. (2013). Substituting the JPL RL06 monthly gravity field product has a negligible effect, and the impact of the selected ocean mask and GIA model is discussed by Uebbing et al. (2019). When replacing the GRACE C_{20} with the GSFC recommended and TN11 solutions, we obtain ocean mass trends and goodness of fit uncertainties of 2.31 ± 0.07 mm/year and 2.23 ± 0.07 mm/year, respectively. Adding these results to the steric estimate, we determine GMSL totals of 3.62±0.21 mm/year using the recommended C_{20} and 3.54±0.21 mm/year using the TN11 C_{20}. Closure of the global sea level budget trends is achieved within uncertainties for both solutions, but we note the improved agreement when the recommended C_{20} product is applied.

For additional validation we consider the recent GRACE-independent inventory of AIS mass fluxes of Gardner et al. (2018), which reports an average mass change of -183 ± 94 Gt/year over the span 2008–2015. Replacing the GRACE C_{20} with our recommended and TN11 C_{20} solutions, we report mass trends and goodness of fit uncertainties of -148.4 ± 5.5 Gt/year and -133.1 ± 5.1 Gt/year, respectively, once again achieving improved agreement when using the recommended C_{20} product. We note that the selected GIA model has a significant impact on GRACE-derived mass changes in AIS (Shepherd et al., 2018) and that our reported values have applied the IJ05_R2 model (Ivins et al., 2013) following several previous studies (Luthcke et al., 2013; Loomis et al., 2019; Shepherd et al., 2012).

As a final validation we compare the 2005–2015 annual signals of the geodetic LOD inferred from the GSFC recommended and TN11 C_{20} solutions to the astrometric LOD following the procedures in Bourda (2008). The astrometric LOD is determined by removing the zonal tides and the atmosphere and ocean angular momentum motion terms from the observed LOD. We note the varied LOD annual amplitudes reported in the literature and speculate that this is due to the different filtering and regression strategies applied to remove the low-frequency astrometric LOD signal (mainly due to core-mantle coupling) and estimate the annual signal. To mitigate the effect of the filter design, we apply wavelet multiresolution analysis to isolate the annual signal and determine its amplitude and phase (Loomis & Luthcke, 2014), resulting in values of [40.0 μs, −133.4°], [46.8 μs, −132.7°], and [59.4 μs, −129.6°], for the astrometric LOD, GSFC geodetic LOD, and TN11 geodetic LOD, respectively (the phase, ϕ, corresponds to $\sin(\omega(t - t_0) + \phi)$, where t_0 is January 1). The better agreement for GSFC geodetic LOD further supports our claim of an improved C_{20} solution.

4. Conclusions

We have applied a systematic approach toward understanding the disparate C_{20} trends of previously published SLR-derived gravity estimates and establishing a recommended methodology and C_{20} data product, where the new product improves the accuracy of GRACE data applications due to its reliance on SLR for the determination of C_{20}. We have demonstrated that the differences between the commonly applied CSR TN11 solution and the GSFC recommended solution are due to the selected arc length and especially the inclusion of GRACE-derived TVG in the forward model. The presented analysis of SLR $\rho_{C_{40}}^{C_{20}}$ values and the accuracy of GRACE C_{40} estimates both provide strong justification for including TVG in the forward model and excluding C_{60} from the set of adjusted parameters. Though several other processing centers have applied TVG when processing SLR measurements, the significance of this design choice was not understood, as no previous effort sought to identify the sources of the C_{20} trend discrepancies despite its significant effect on GMSL, AIS, and GIS mass change estimates. In addition to improving the accuracy of GRACE and GRACE-FO applications, an improved C_{20} estimate should also benefit the application and interpretation of previously developed methods (e.g., Bonin et al., 2018; Nerem & Wahr, 2011) that seek to leverage the high spatial resolution of GRACE/GRACE-FO and the longer, continuous data record of SLR.

Acknowledgments
Support for this work was provided by the NASA GRACE and GRACE Follow-On Science Team Grant NNH15ZDA001N. SLR normal point data are from CDDIS, a global data center for the International Laser Ranging Service (ILRS; https://cddis.nasa.gov). Atmospheric loading corrections are provided by the EOST Loading Service (http://loading.u-strasbg.fr/). Length-of-day data are provided by the International Earth Rotation and Reference Systems Service (IERS; https://www.iers.org). Atmospheric and ocean angular momentum products are provided by Helmholtz-Zentrum Potsdam – Deutches GeoForschungsZentrum (GFZ; ftp://esmdata.gfz-potsdam.de/EAM). We acknowledge the expertise of our colleagues F. G. Lemoine, N. P Zelensky, and D. S. Chinn, whose prior work was foundational to this study. The recommended GSFC C_{20} solution is available for download at https://neptune.gsfc.nasa.gov/slr_tvg/.

References

Bloßfeld, M., Müller, H., Gerstl, M., Štefka, V., Bouman, J., Göttl, F., & Horwath, M. (2015). Second-degree stokes coefficients from multi-satellite slr. *Journal of Geodesy*, *89*(9), 857–871. https://doi.org/10.1007/s00190-015-0819-z

Böckmann, S., Artz, T., & Nothnagel, A. (2010). VLBI terrestrial reference frame contributions to ITRF2008. *Journal of Geodesy*, *84*(3), 201–219. https://doi.org/10.1007/s00190-009-0357-7

Bonin, J. A., Chambers, D. P., & Cheng, M. (2018). Using satellite laser ranging to measure ice mass change in Greenland and Antarctica. *The Cryosphere*, *12*, 71–79.

Bourda, G. (2008). Length-of-day and space-geodetic determination of the Earth's variable gravity field. *Journal of Geodesy*, *82*(4), 295–305. https://doi.org/10.1007/s00190-007-0180-y

Chen, J. L., Wilson, C. R., & Seo, K.-W. (2009). S2 tide aliasing in grace time-variable gravity solutions. *Journal of Geodesy*, *83*(7), 679–687. https://doi.org/10.1007/s00190-008-0282-1

Cheng, M., & Ries, J. (2017). The unexpected signal in grace estimates of c20. *Journal of Geodesy*, *91*(8), 897–914. https://doi.org/10.1007/s00190-016-0995-5

Cheng, M., Tapley, B. D., & Ries, J. C. (2013). Deceleration in the Earth's oblateness. *Journal of Geophysical Research: Solid Earth*, *118*, 740–747. https://doi.org/10.1002/jgrb.50058

Flechtner, F. (2007). AOD1B product description document for product release 05. http://www.gfz-potsdam.de/en/aod1b/, GRACE Project Document 327-750.

Förste, C., Bruinsma, S., O., A., Rudenko, S., Lemoine, J.-M., Marty, J.-C., et al. (2016). EIGEN-6S4 A time-variable satellite-only gravity field model to d/o 300 based on LAGEOS, GRACE and GOCE data from the collaboration of GFZ Potsdam and GRGS Toulouse v. 2.0.http://doi.org/10.5880/icgem.2016.008, GFZ Data Services.

Gardner, A. S., Moholdt, G., Scambos, T., Fahnstock, M., Ligtenberg, S., van den Broeke, M., & Nilsson, J. (2018). Increased west antarctic and unchanged east antarctic ice discharge over the last 7 years. *The Cryosphere*, *12*(2), 521–547.

Geruo, A., Wahr, J., & Zhong, S. (2013). Computations of the viscoelastic response of a 3-D compressible Earth to surface loading: an application to Glacial Isostatic Adjustment in Antarctica and Canada. *Geophysical Journal International*, *192*(2), 557–572. https://doi.org/10.1093/gji/ggs030

Group, WCRP Global Sea Level Budget (2018). Global sea-level budget 1993–present. *Earth System Science Data*, *10*(3), 1551–1590.

Hsu, C.-W., & Velicogna, I. (2017). Detection of sea level fingerprints derived from grace gravity data. *Geophysical Research Letters*, *44*, 8953–8961. https://doi.org/10.1002/2017GL074070

Ivins, E. R., James, T. S., Wahr, J., O'Schrama, E. J., Landerer, F. W., & Simon, K. M. (2013). Antarctic contribution to sea level rise observed by grace with improved GIA correction. *Journal of Geophysical Research: Solid Earth*, *118*, 3126–3141. https://doi.org/10.1002/jgrb.50208

Jin, S., Zhang, L. J., & Tapley, B. D. (2011). The understanding of length-of-day variations from satellite gravity and laser ranging measurements. *Geophysical Journal International*, *184*(2), 651–660. https://doi.org/10.1111/j.1365-246X.2010.04869.x

Johnson, G. C., & Chambers, D. P. (2013). Ocean bottom pressure seasonal cycles and decadal trends from grace release-05: Ocean circulation implications. *Journal of Geophysical Research: Oceans*, *118*, 4228–4240. https://doi.org/10.1002/jgrc.20307

Klinger, B., & Mayer-Gürr, T. (2016). The role of accelerometer data calibration within grace gravity field recovery: Results from itsg-grace2016. *Advances in Space Research*, *58*(9), 1597–1609.

Lemoine, J.-M., Bourgogne, S., Biancale, R., & Bruinsma, S. (2018). Rl04 monthly gravity field solutions from CNES/GRGS. http://presentations.copernicus.org/GSTM-2018-42_presentation.pdf, GRACE/GRACE-FO Science Team Meeting, Potsdam, Germany.

Lemoine, J.-M., Bruinsma, S., Loyer, S., Biancale, R., Marty, J.-C., Perosanz, F., & Balmino, G. (2007). Temporal gravity field models inferred from grace data. *Advances in Space Research*, *39*(10), 1620–1629.

Lemoine, F. G., Klosko, S. M., Cox, C. M., & Johnson, T. J. (2006). Time-variable gravity from SLR and DORIS tracking. https://cddis.nasa.gov/lw15/, 15th International workshop on laser ranging, Canberra.

Leuliette, E. W., & Willis, J. K. (2011). Balancing the sea level budget. *Oceanography*, *24*, 122–129. https://doi.org/10.5670/oceanog.2011.32

Loomis, B. D., & Luthcke, S. B. (2014). Optimized signal denoising and adaptive estimation of seasonal timing and mass balance from simulated GRACE-like regional mass variations. *Advances in Adaptive Data Analysis*, *06*(01), 1450003. https://doi.org/10.1142/S1793536914500034

Loomis, B. D., Luthcke, S. B., & Sabaka, T. J. (2019). Regularization and error characterization of grace mascons. *Journal of Geodesy*. https://doi.org/10.1007/s00190-019-01252-y

Luthcke, S. B., Sabaka, T. J., Loomis, B. D., Arendt, A. A., McCarthy, J. J., & Camp, J. (2013). Antarctica, Greenland and Gulf of Alaska land-ice evolution from an iterated GRACE global mascon solution. *Journal of Glaciology*, *59*(216), 613–631.

Meyer, U., Jäggi, A., & Beutler, G. (2012). Monthly gravity field solutions based on grace observations generated with the celestial mechanics approach. *Earth and Planetary Science Letters*, *345-348*, 72–80.

Nerem, R. S., & Wahr, J. (2011). Recent changes in the Earth's oblateness driven by Greenland and Antarctic Ice Mass loss. *Geophysical Research Letters*, *38*, L13501. https://doi.org/10.1029/2011GL047879

Otsubo, T., & Appleby, G. M. (2003). System-dependent center-of-mass correction for spherical geodetic satellites. *Journal of Geophysical Research*, *108*(B4), 2201. https://doi.org/10.1029/2002JB002209

Otsubo, T., Sherwood, R. A., Appleby, G. M., & Neubert, R. (2015). Center-of-mass corrections for sub-cm-precision laser-ranging targets: Starlette, Stella and LARES. *Journal of Geodesy*, *89*(4), 303–312. https://doi.org/10.1007/s00190-014-0776-y

Pail, R., Goiginger, H., Schuh, W.-D., Höck, E., Brockmann, J. M., Fecher, T., et al. (2010). Combined satellite gravity field model GOCO01s derived from GOCE and GRACE. *Geophysical Research Letters*, *37*, L20314. https://doi.org/10.1029/2010GL044906

Petit, G., & Luzum, B. (Eds.) (2010). *IERS conventions (2010)*. https://www.iers.org/IERS/EN/Publications/TechnicalNotes/tn36.html, (IERS Technical Note 36) Frankfurt am Main: Verlag des Bundesamts für Kartographie und Geodäsie, ISBN 3-89888-989-6.

Petrov, L., & Boy, J.-P. (2004). Study of the atmospheric pressure loading signal in very long baseline interferometry observations. *Journal of Geophysical Research*, *109*, B03405. https://doi.org/10.1029/2003JB002500

Ray, R. (1999). A global ocean tide model from TOPEX/POSEIDON altimetry: GOT99.2. https://denali.gsfc.nasa.gov/personal_pages/ray/MiscPubs/19990089548_19%99150788.pdf, NASA Tech. Memo 209478.

Ray, R. D., & Luthcke, S. B. (2006). Tide model errors and GRACE gravimetry: Towards a more realistic assessment. *Geophysical Journal International*, *167*(3), 1055–1059. https://doi.org/10.1111/j.1365-246X.2006.03229.x

Ries, J. C., & Desai, S. (2017). Update to the conventional model for rotational deformation. AGU Fall Meeting.

Save, H., Bettadpur, S., & Tapley, B. D. (2016). High-resolution CSR GRACE RL05 mascons. *Journal of Geophysical Research: Solid Earth*, *121*, 7547–7569. https://doi.org/10.1002/2016JB013007

Seo, K. W., Wilson, C. R., Han, S. C., & Waliser, D. E. (2008). Gravity recovery and climate experiment (GRACE) alias error from ocean tides. *Journal of Geophysical Research*, *113*, B03405. https://doi.org/10.1029/2006JB004747

Shepherd, A., Ivins, E. R., Geruo, A., Barletta, V. R., Bentley, M. J., Bettadpur, S., et al. (2012). A reconciled estimate of ice-sheet mass balance. *Science*, *338*(6111), 1183–1189.

Shepherd, A., Ivins, E., Rignot, E., Smith, B., van den Broeke, M., Velicogna, I., et al. (2018). Mass balance of the antarctic ice sheet from 1992 to 2017. *Nature*, *558*(7709), 219–222.

Sośnica, K., Jäggi, A., Meyer, U., Thaller, D., Beutler, G., Arnold, D., & Dach, R. (2015). Time variable Earth's gravity field from SLR satellites. *Journal of Geodesy*, *89*(10), 945–960. https://doi.org/10.1007/s00190-015-0825-1

Talpe, M. J., Nerem, R. S., Forootan, E., Schmidt, M., Lemoine, F. G., Enderlin, E. M., & Landerer, F. W. (2017). Ice mass change in Greenland and Antarctica between 1993 and 2013 from satellite gravity measurements. *Journal of Geodesy*, *91*(11), 1283–1298. https://doi.org/10.1007/s00190-017-1025-y

Uebbing, B., Kusche, J., Rietbroek, R., & Landerer, F. W. (2019). Processing choices affect ocean mass estimates from GRACE. *Journal of Geophysical Research: Oceans*, *124*, 1029–1044. https://doi.org/10.1029/2018JC014341

Wahr, J., Swenson, S., & Velicogna, I. (2006). Accuracy of GRACE mass estimates. *Geophysical Research Letters*, *33*, L06401. https://doi.org/10.1029/2005GL025305

Watkins, M. M., Wiese, D. N., Yuan, D.-N., Boening, C., & Landerer, F. W. (2015). Improved methods for observing Earth's time variable mass distribution with grace using spherical cap mascons. *Journal of Geophysical Research: Solid Earth*, *120*, 2648–2671. https://doi.org/10.1002/2014JB011547

Yu, N., Li, J., Ray, J., & Chen, W. (2018). Improved geophysical excitation of length-of-day constrained by Earth orientation parameters and satellite gravimetry products. *Geophysical Journal International*, *214*(3), 1633–1651. https://doi.org/10.1093/gji/ggy204

Zelensky, N. P., Lemoine, F. G., Chinn, D. S., Melachroinos, S., Beckley, B. D., Beall, J. W., & Bordyugov, O. (2014). Estimated SLR station position and network frame sensitivity to time-varying gravity. *Journal of Geodesy*, *88*(6), 517–537. https://doi.org/10.1007/s00190-014-0701-4